Keratin 8 phosphorylation regulates its transamidation and hepatocyte Mallory-Denk body formation

Raymond Kwan,[*,1,2] Shinichiro Hanada,[†,1] Masaru Harada,[‡,1] Pavel Strnad,[§] Daniel H. Li,[‖] and M. Bishr Omary[*]

[*]Department of Molecular and Integrative Physiology, University of Michigan Medical School, Ann Arbor, Michigan, USA; [†]Division of Gastroenterology, Department of Medicine, Kurume University School of Medicine, Kurume, Japan; [‡]Third Department of Internal Medicine, University of Occupational and Environmental Health, School of Medicine, Kitakyushu, Japan; [§]Department of Internal Medicine I, University of Ulm, Ulm, Germany; and [‖]AnaSpec, Fremont, California, USA

ABSTRACT **Mallory-Denk bodies (MDBs) are hepatocyte inclusions that are associated with poor liver disease prognosis. The intermediate filament protein keratin 8 (K8) and its cross-linking by transglutaminase-2 (TG2) are essential for MDB formation. K8 hyperphosphorylation occurs in association with liver injury and MDB formation, but the link between keratin phosphorylation and MDB formation is unknown. We used a mutational approach to identify K8 Q70 as a residue that is important for K8 cross-linking to itself and other liver proteins. K8 cross-linking is markedly enhanced on treating cells with a phosphatase inhibitor and decreases dramatically on K8 S74A or Q70N mutation in the presence of phosphatase inhibition. K8 Q70 cross-linking, in the context of synthetic peptides or intact proteins transfected into cells, is promoted by phosphorylation at K8 S74 or by an S74D substitution and is inhibited by S74A mutation. Transgenic mice that express K8 S74A or a K8 G62C liver disease variant that inhibits K8 S74 phosphorylation have a markedly reduced ability to form MDBs. Our findings support a model in which the stress-triggered phosphorylation of K8 S74 induces K8 cross-linking by TG2, leading to MDB formation. These findings may extend to neuropathies and myopathies that are characterized by intermediate filament-containing inclusions.—Kwan, R., Hanada, S., Harada, M., Strnad, P., Li, D. H., Omary, M.B. Keratin 8 phosphorylation regulates its transamidation and hepatocyte Mallory-Denk body formation. *FASEB J.* 26, 2318–2326 (2012). www.fasebj.org**

Key Words: intermediate filaments · steatohepatitis · transglutaminase 2

Several human liver diseases, particularly steatohepatitis but also other entities, such as viral hepatitis, are associated with prominent intracytoplasmic inclusions termed Mallory-Denk bodies (MDBs) (1, 2). The presence of MDBs serves as a poor prognostic marker in patients with liver disease (3–5). MDBs are primarily composed of the intermediate filament (IF) proteins keratins 8 and 18 (K8/K18), as well as ubiquitin (Ub) and the Ub-binding protein p62 (1, 2, 6). K8 and K18 exist as obligate noncovalent heteropolymers in a 1:1 stoichiometry and form cytoplasmic filaments that provide structural support and cytoprotective functions in hepatocytes (2).

MDB formation can be induced in mice through chronic feeding with griseofulvin or 3,5-diethoxycarbonyl-1,4-dihydrocollidine (DDC) (7, 8). These mouse models, coupled with the use of transgenic mice that overexpress K8 and/or K18 and mice with null alleles of these genes, have helped elucidate the molecular requirements for MDB formation. Therefore, it is now clear that K8 is particularly important for MDB formation, because K8-null mice do not develop MDB in response to DDC feeding, in contrast to K18-null animals, which develop spontaneous MDBs on aging (9, 10). In addition, transgenic mice that overexpress K8 develop MDBs spontaneously (without DDC feeding) on aging, while K18-overexpressing mice are highly resistant to MDB formation despite DDC feeding (11, 12). Thus, an increase in hepatocyte K8 levels relative to K18, which occurs in the context of some forms of liver injury, is critical for MDB formation. Biophysical studies further support the importance of K8 in MDB formation. For example, K8, but not K18, acquires a cross-β-sheet structure (a defining feature of amyloid inclusion proteins) on MDB formation, suggesting that K8 conformational changes and aggregation are likely drivers of MDB formation (13–16).

Abbreviations: BHK, baby hamster kidney; CHO, Chinese hamster ovary; DDC, 3,5 diethoxycarbonyl-1,4-dihydrocollidine; H&E, hematoxylin and eosin; IF, intermediate filament; K8, keratin 8; K18, keratin 18; MDB, Mallory-Denk body; OA, okadaic acid; TG, transglutaminase; TG2, transglutaminase-2; Ub, ubiquitin; WME, William's medium E; WT, wild type

[1] These authors contributed equally to this work.

[2] Correspondence: Department of Molecular and Integrative Physiology, 7744 Medical Science Bldg. II, 1301 E. Catherine, Ann Arbor, MI 48109-0622, USA. E-mail: raykwan@umich.edu

doi: 10.1096/fj.11-198580

This article includes supplemental data. Please visit *http://www.fasebj.org* to obtain this information.

0892-6638/12/0026-2318 © FASEB

In MDBs, both K8 and K18 are covalently linked to other MDB-constituent proteins by transglutaminases (TGs), calcium-dependent transamidating enzymes that cross-link proteins *via* amide bonds between the ε-amino group of lysine and the γ-carboxyl group of glutamine (17–19). TG2 is the most abundant TG activity in the liver and has been implicated in the cross-linking of various inclusion-constituent proteins, including mutant huntingtin in Huntington disease (20–24) and α-synuclein in Parkinson disease (25, 26). Notably, K8 is the preferred substrate for TG2 as compared with K18, and the TG2-mediated cross-linking of K8 to other MDB-constituent proteins is essential for MDB formation since TG2-null mice are highly resistant to DDC-induced MDB formation (27). The potent TG2 inhibitor KCC009 prevents DDC-induced mouse hepatomegaly but not MDB formation, but it is unclear whether KCC009 can inhibit intracellular TG2 activity *in vivo* (28), which is required for MDB formation. Phosphokeratins (*e.g.*, K8 pS24, pS74, and pS432), particularly K8 pS74, are prominent within human and mouse MDBs (29), but the connection between keratin phosphorylation, cross-linking, and MDB formation is unknown.

In the current study, we first focused on identifying K8 transamidation sites, given the importance of K8 transamidation in MDB formation. This led us to identify K8 Q70 as a preferential transamidation site in K8 and to show that K8 S74 phosphorylation not only promotes keratin cross-linking but is also critical for MDB formation in mice. These findings provide the first direct link between keratin phosphorylation and MDB formation and characterize the first K8 glutamine transamidation site.

MATERIALS AND METHODS

Mice

Three transgenic mouse lines that overexpress K8 wild type (WT), K8 G62C, and K8 S74A (all in an FVB genetic background) were described previously (30). Genotyping was performed by PCR screening using mouse tail genomic DNA as described previously (30). All mice received humane care in compliance with the U.S. Department of Health and Human Services Guide for the Care and Use of Laboratory Animals, and their use was approved by the University Committee on Use and Care of Animals (UCUCA) at the University of Michigan.

DDC treatment and tissue harvesting

Mice were fed a powdered chow (Formulab Diet 5008; Deans Animal Feeds, Redwood City, CA, USA) containing 0.1% DDC (Sigma-Aldrich, St. Louis, MO, USA) for 6 wk, which results in readily detectable MDBs in the K8 WT-overexpressing mice (11, 12). At the conclusion of the feeding period, mice were sacrificed by CO_2 inhalation, and tissue harvesting was performed as described previously (11).

Antibodies

The following antibodies were used: rabbit anti-mouse/human (h) TG2 and mouse anti-hK8 mAb (M20 and TS1; Lab Vision, Fremont, CA, USA), rat anti-mouse/human K8 mAb (Troma I; Developmental Studies Hybridoma Bank, Iowa City, IA, USA); rabbit anti-K8/18 Ab-8592; rabbit anti-K18 Ab-4668; and mouse anti-Ub mAb (Santa Cruz Biotechnology, Santa Cruz, CA, USA).

Immunofluoresence staining

Livers were sectioned and fixed with −20°C acetone (10 min). Staining was carried out as described previously (31). Images were obtained using a 60×/NA 1.40 water lens or a 20×/NA 1.40 lens combined with a confocal microscope (Zeiss 510 Meta, Carl Zeiss, Thornwood, NY, USA), and acquired by LaserSharp software (Carl Zeiss, Thornwood, NY, USA). For double-labeling analyses, images were acquired sequentially using separate excitation wavelengths of 488 nm for fluorescein thiocyanate or Alexa 488 and 568 nm for Texas red, and then merged.

Gel electrophoresis and immunoblotting

Liver tissues were lysed in homogenization buffer (0.187 M Tris-HCl, pH 6.8; 3% SDS; 5 mM EDTA). Homogenates were diluted with 4× reducing Laemmli sample buffer, and equal amounts of protein were applied to SDS-PAGE, followed by blotting and visualization of the immune-reactive species using Western Lightning-ECL (GE Healthcare, Piscataway, NJ, USA).

Histological analysis

Hematoxylin and eosin (H&E)-stained sections were assessed for the histological criteria of hepatocyte ballooning, MDB formation, and ductal proliferation using 0–3 scoring (0, none; 1, rare; 2, frequent; 3, abundant). Scheuer's criteria were applied for the analysis of liver inflammation and necrosis (32).

In vitro analysis for cross-linking of K8

Baby hamster kidney (BHK) cells were transfected with an equal amount of human K8 WT, K8 Q7N, K8 Q70N, K8 S74A, K8 S74D, K8 Q85N, K8 Q85N Q90N, or Q408N plasmid together with K18 WT using Lipofectamine 2000 (Invitrogen, Carlsbad, CA, USA). In some cases, cells were treated with 1 μM okadaic acid (OA; Enzo Life Sciences, Farmingdale, NY, USA). After 48 h, the transfected cells were lysed in Nonidet P-40 buffer [1% Nonidet P-40, 1× PBS (pH 7.4), 5 mM EDTA, and protease inhibitor cocktail from Sigma-Aldrich], and equal volumes of extracts were incubated with 3.5 μg/ml recombinant TG2 in the presence of 15 mM $CaCl_2$ (37°C). The reaction was quenched by adding 4× reducing Laemmli sample buffer, followed by gel electrophoresis and immunoblotting.

Hepatocyte isolation

Male mice were used. After anesthesia, the liver was first perfused with a buffer containing Hanks' balanced salt solution that includes 0.5 mM EGTA, 5.5 mM glucose, and 1% penicillin-streptomycin. This was followed by perfusion with a collagenase IV (Worthington, Lakewood, NJ, USA) containing buffer that includes Hanks' balanced salt solution with 1.2 mM $CaCl_2$ and 5.5 mM glucose, 1% penicillin-streptomycin. The cells were then dispersed in William's medium E (WME), filtered through a 70-μm cell strainer, pelleted (500 rpm, 2 min, 4°C), and washed twice before plating at a density of 5 ×

10^5 cells/ml on collagen I-coated plates (BD BioCoat; BD Biosciences, Bedford, MA, USA) in WME supplemented with 10% FBS and 1% penicillin-streptomycin. After 1 h, the culture medium was replaced, and cells were allowed to attach for another 12 h (37°C, 5% CO_2) before OA treatment. All of the solutions were prewarmed to 37°C before use.

In vitro cross-linking of K8 peptides to mouse liver proteins

Biotin-tagged peptides spanning K8 Ala65 to Lys81 were synthesized using standard methods (AnaSpec, Fremont, CA, USA). The synthesized peptides represented K8 WT, pS74 (phosphopeptide), and D74 (phosphomimetic peptide). As a glutamine control peptide, a biotin-tagged K8 peptide containing Q85 (K8 Q85) was generated as a negative control. Peptides (1.4 mM) were incubated (37°C) with Nonidet P-40 lysates from normal mouse livers, followed by the addition of TG2 (3.5 μg/ml) in the presence of 15 mM $CaCl_2$ (2 h). The reaction was quenched by adding 4× reducing Laemmli sample buffer, followed by gel electrophoresis and blotting using streptavidin-HRP (KPL, Gaithersburg, MD, USA).

Stable Chinese hamster ovary (CHO) cell line selection and MG132/peroxide treatments

CHO cells were cultured in DMEM supplemented with 10% FBS and 1% penicillin/streptomycin. Cells were transfected with the following pcDNA 3 (Invitrogen) constructs: WT K18 plus either WT K8, Q70N K8, or Q85N K8. Stably transfected cells were selected using 600 μg/ml geneticin. Clones expressing K18 and K8 were isolated by limiting dilution and tested for keratin expression and filament organization by immunofluorescence staining. MG132 (5 μM; EMD Chemicals, Gibbstown, NJ, USA), and H_2O_2 (1.2 mM) stock solutions were used as specified in the figure legend.

Statistical analysis

Values are shown as means ± SD. Student's *t* test and Spearman rank correlation were used, with $P < 0.05$ being considered significant.

RESULTS

Identification of Q70 as a human K8 transamidation site

We used site-directed mutagenesis to identify glutamine and lysine residues in K8 as potential TG2 target sites. For this purpose, K8 Gln→Asn and Lys→Arg mutants at potential transamidation sites were generated in the head and tail domains of K8 (**Fig. 1*A***). We focused on head and tail domains because they are the domains that include hitherto well-characterized post-translational modifications, while modifications in the rod domains of IF proteins are generally uncommon (33). BHK cells, which do not express endogenous K8 or K18, were cotransfected with WT or mutant K8 and WT K18. Efficient expression of K8 for the Q→N mutants (Fig. 1*B*) and K→R mutants (Supplemental Fig. S1) was confirmed. We then developed an *in vitro* TG assay to compare the TG2-mediated cross-linking of WT K8 with that of the Q→N and K→R mutants.

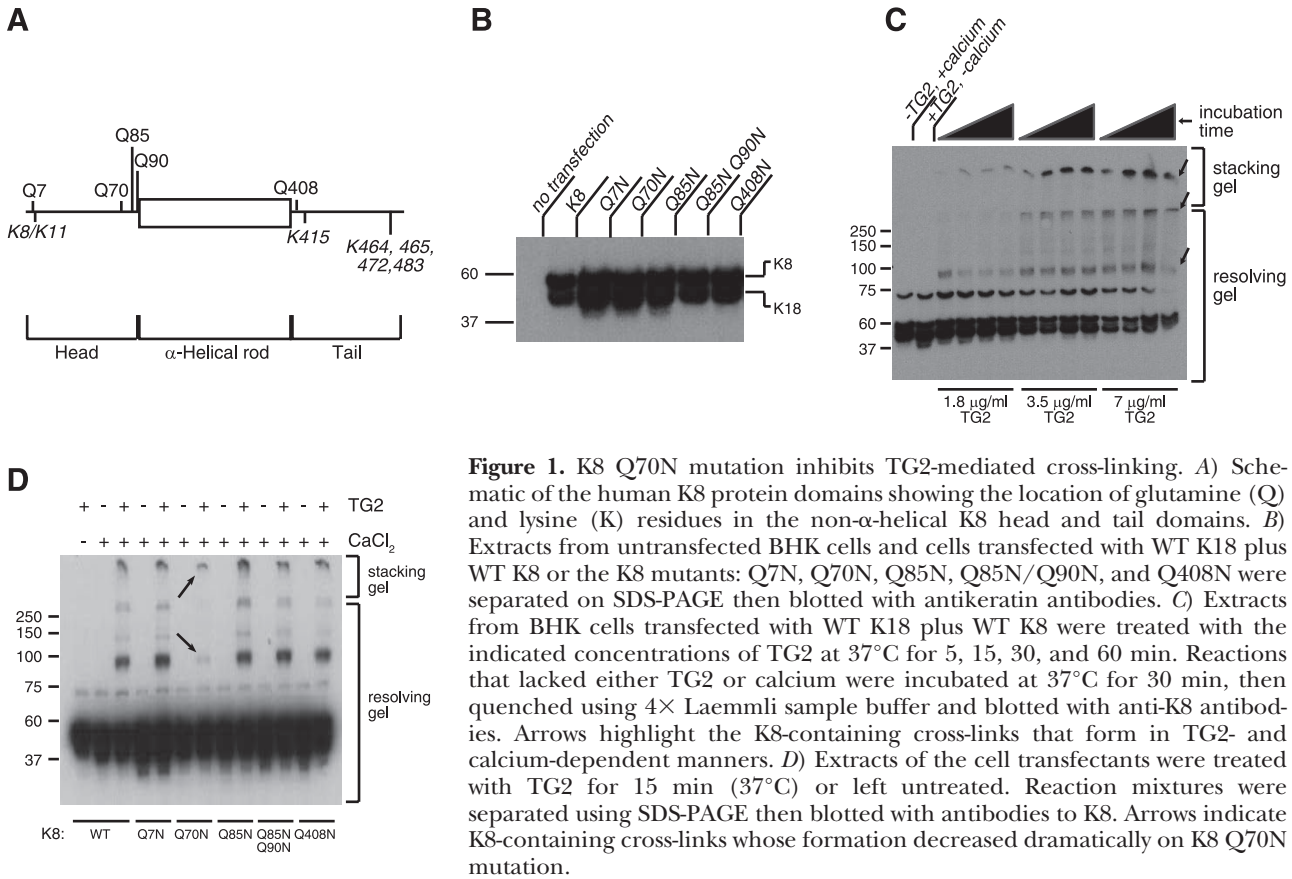

Figure 1. K8 Q70N mutation inhibits TG2-mediated cross-linking. *A*) Schematic of the human K8 protein domains showing the location of glutamine (Q) and lysine (K) residues in the non-α-helical K8 head and tail domains. *B*) Extracts from untransfected BHK cells and cells transfected with WT K18 plus WT K8 or the K8 mutants: Q7N, Q70N, Q85N, Q85N/Q90N, and Q408N were separated on SDS-PAGE then blotted with antikeratin antibodies. *C*) Extracts from BHK cells transfected with WT K18 plus WT K8 were treated with the indicated concentrations of TG2 at 37°C for 5, 15, 30, and 60 min. Reactions that lacked either TG2 or calcium were incubated at 37°C for 30 min, then quenched using 4× Laemmli sample buffer and blotted with anti-K8 antibodies. Arrows highlight the K8-containing cross-links that form in TG2- and calcium-dependent manners. *D*) Extracts of the cell transfectants were treated with TG2 for 15 min (37°C) or left untreated. Reaction mixtures were separated using SDS-PAGE then blotted with antibodies to K8. Arrows indicate K8-containing cross-links whose formation decreased dramatically on K8 Q70N mutation.

As shown in Fig. 1*C*, treatment of Nonidet P-40 extracts of K8-expressing BHK cells with increasing amounts of recombinant TG2 or with increasing incubation times resulted in increasing amounts of K8 cross-linking that is detected at the top of the stacking gel or at the interface of the stacking and resolving gel (Fig. 1*C*). K8 cross-linking is dependent on both TG2 and its cofactor calcium, as no cross-linking was observed without both TG2 and calcium in the reaction (Fig. 1*C*).

After establishing the *in vitro* transamidation assay conditions, we compared TG2-mediated transamidation of WT K8 to that of K→R and Q→N mutant K8 proteins. The K→R K8 mutant proteins exhibited relatively similar levels of K8 cross-linking after TG2 treatment (Supplemental Fig. S1*B*), which is consistent with reports that TG2 substrate specificity is determined primarily by the amino acid sequence flanking the glutamine residues rather than the lysine residues of potential substrates (34). In contrast, all Q→N mutant K8 proteins had a level of cross-linking that is similar to WT K8 except for K8 Q70N, which exhibited a significant impairment in K8 cross-linking (Fig. 1*D*, arrows).

The findings of the *in vitro* transamidation assay suggest that Q70 in K8 is important for the TG2-mediated cross-linking of K8, and potentially for subsequent MDB formation. To test this hypothesis in the context of live cells, CHO cells, which do not express endogenous keratins, were stably transfected with WT K8, Q70N K8, and Q85N K8, and clones expressing these proteins were isolated. MDB formation is initiated in response to increased oxidative stress and the accumulation of unfolded or damaged proteins within the cell (2, 35–39). Also, oxidative stress has been shown to increase TG2 activity (40–42). To mimic these conditions in cell culture, WT-, Q70N-, and Q85N K8-expressing clones were treated with H_2O_2 and/or the proteasome inhibitor MG132. Such treatments of the WT or Q85N K8 clones caused the appearance of a highly cross-linked species of K8 (**Fig. 2*A***), while the Q70N mutation prevented the appearance of cross-linked K8 after H_2O_2 ± MG132 treatments, despite the somewhat higher level of Q70N K8 relative to WT and Q85N clones after treatment (Fig. 2*A*).

K8 site-specific phosphorylation enhances TG2-mediated K8 cross-linking

The results shown in Figs. 1*D* and 2*A* suggest that Q70 in K8 is a TG2 substrate. Notably, Q70 is in close

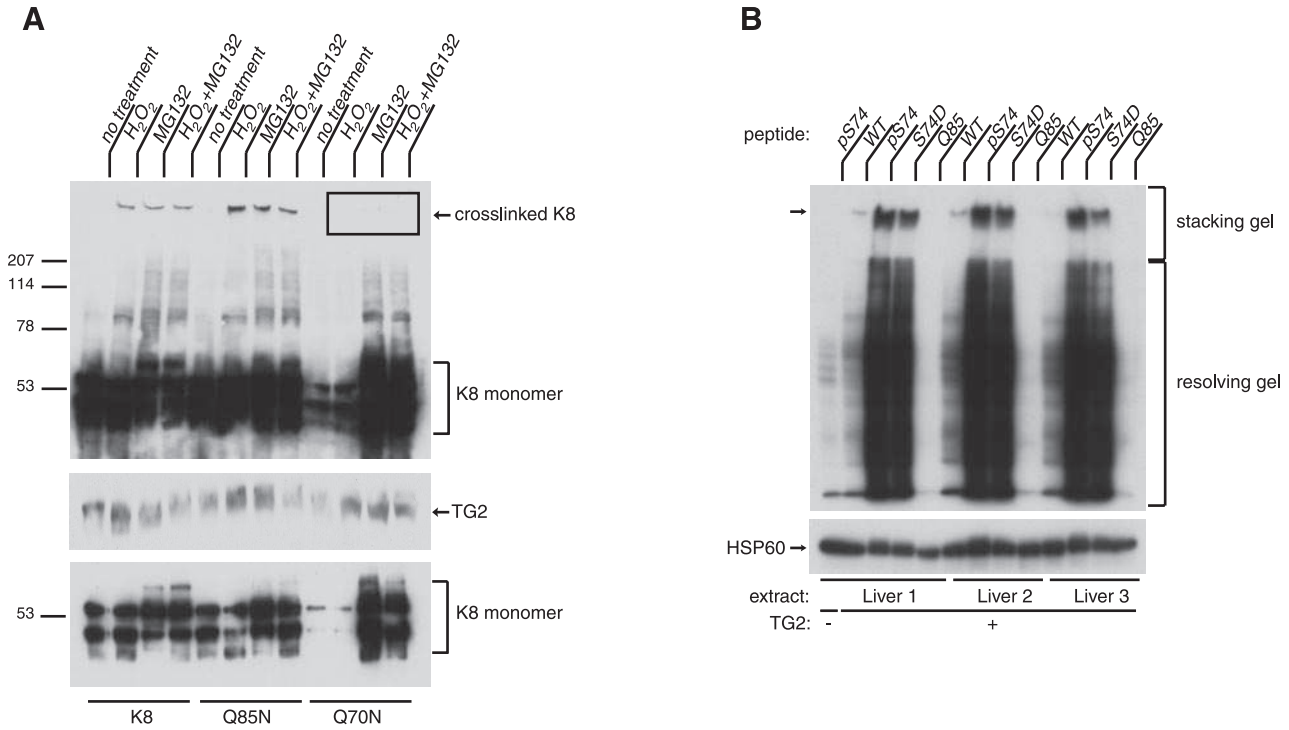

Figure 2. K8 S74 phosphorylation enhances Q70 transamidation *in vitro*. *A*) CHO cells stably transfected with K8 WT, K8 Q85N, and K8 Q70N were treated with vehicle or with 5 μM MG132 and/or 1.2 mM H_2O_2 for 24 h. Cells were lysed in homogenization buffer, and extracts were blotted with antibodies to TG2 (middle panel) or to K8 (upper and lower panels, with lower panel being a lighter exposure to show the relative intensity of the K8 monomeric species). *B*) Biotinylated peptides K8 WT, K8 pS74, and K8 S74D (all 3 peptides contain Q70 and are identical except for having S74, pS74, and D74) and the glutamine control peptide K8 WT-Q85 (see Table 1 for sequences) were incubated (37°C) with Nonidet P-40 lysates from normal mouse liver and TG2 (3.5 μg/ml) in the presence of 15 mM $CaCl_2$ for 2 h. Three independent liver lysates were tested. Reaction was quenched by adding 4× reducing sample buffer, followed by separation using SDS-PAGE, then immune blotting with streptavidin-HRP to visualize liver proteins that became cross-linked to the biotinylated peptides. Arrow indicates biotinylated K8 peptide that becomes cross-linked to liver proteins to generate high-molecular-weight species, aside from the range of other cross-linked adducts.

TABLE 1. *K8 biotinylated peptide sequences*

Peptide	Sequence
K8 WT	AVTVNQSLLSPLVRRK-biotin
K8 pS74	AVTVNQSLLpSPLVRRK-biotin
K8 S74D	AVTVNQSLLDPLVRRK-biotin
K8 WT-Q85	VDPNIQAVRTNERRRK-biotin

Gln and S74 residues are underscored. See Fig. 2*B*.

proximity to S74 in K8, which is not phosphorylated in normal hepatocytes but becomes phosphorylated in human and mouse MDBs (29) or on exposure of epithelial cells and tissues to a wide range of stresses (33). We compared the amino acid sequence flanking Q70 with reported TG2 transamidation consensus sequences. One reported consensus sequence (34), QXXφDP, is similar to the amino acid sequence flanking Q70 (QSLLSP), except that there is a consensus aspartate residue in the position that S74 occupies that could mimic a phospho-S74. Therefore, we hypothesized that S74 phosphorylation acts as a K8 cross-linking switch that converts Q70 from a poor TG2 substrate into a good one. We tested this hypothesis using synthetic K8 biotinylated peptides (**Table 1**) that share Q70 but include either S74, pS74, or D74, and also used a K8 Q85-containing peptide as a control. As shown in Fig. 2*B*, the pS74 and the phosphomimetic D74 peptides are excellent TG2 substrates that are able to cross-link with numerous mouse liver proteins as compared with the WT (*i.e.*, nonphospho-S74 K8) or K8 Q85N control peptides.

We then asked whether overall K8 hyperphosphorylation enhances its TG2-mediated cross-linking. For this, we treated human colon carcinoma HT29 cells, which express high levels of K8 and K18 (31), with the phosphatase inhibitor OA and then tested the cell extracts using an *in vitro* transamidation assay. OA inhibits protein phosphatase (PP) 1, 2A, and 4–6, and to a lesser extent PP 2B and 7 (43), and the treatment of cells with this toxin results in hyperphosphorylation at Ser and Thr residues (44). After 30 and 60 min of OA treatment, K8 became markedly phosphorylated at S74, as determined using a K8 pS74-specific antibody (**Fig. 3*A***). Furthermore, the addition of TG2 to HT29 extracts from untreated cells produced limited, if any,

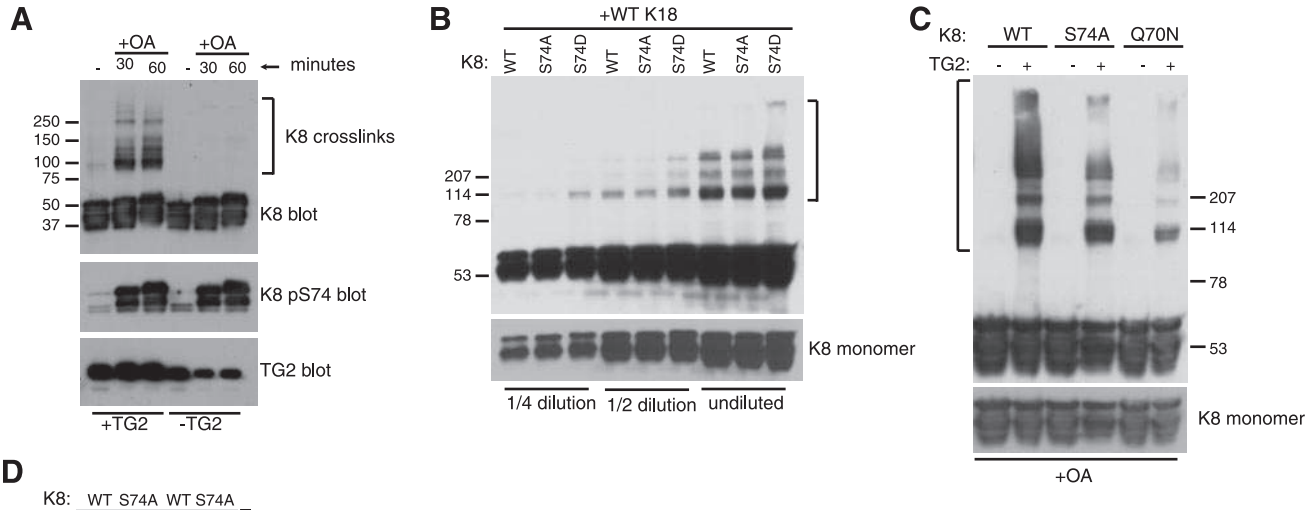

Figure 3. K8 S74A mutation inhibits K8 transamidation by TG2 *in vitro*. *A*) HT29 cells were treated with vehicle or 1 μM OA for 30 or 60 min. Treated cells were solubilized in Nonidet P-40-containing buffer, then incubated with or without TG2 for 15 min (37°C). Extracts were analyzed by blotting, using antibodies to K8, K8 pS74, and TG2. TG2 blot (bottom panel) confirms the addition of exogenous TG2 to the designated extracts. Note that hyperphosphorylation promotes K8-containing cross-link formation. *B*) BHK cells were transfected with WT K18 plus the indicated K8 constructs. After 48 h, cells were solubilized with Nonidet P-40, followed by TG2 reactions (15 min, 37°C) using the undiluted extracts or extracts diluted by 1/2 and 1/4. After quenching, samples were separated by SDS-PAGE, followed by immune blotting using anti-K8 antibodies to assess K8 cross-linking (indicated by bracket). Bottom panel shows a lower exposure of the gel in order to demonstrate near-equal loading. *C*) BHK cells were transfected with WT K18 plus the indicated K8 constructs. After 48 h, OA (1 μM, 30 min) was added to the cultured cells, followed by detergent solubilization. Cell extracts were either left untreated or treated with TG2 for 15 min (37°C), followed by quenching, then analysis of K8 cross-links (indicated by bracket) by immunoblotting with an anti-K8 antibody. Bottom panel shows a lower exposure of the gel in order to demonstrate near-equal loading for each dilution set. *D*) Primary hepatocytes were isolated from K8 S74A and K8 WT transgenic mice; after 8 h of culture, hepatocytes were treated with either DMSO alone or 1 μM OA (45 min, 37°C). Cultured hepatocytes were then lysed in Nonidet P-40 buffer, and extracts were subjected to *in vitro* transamidation. Middle panel shows human K8 expression (input) in the hepatocyte extracts. Bottom panel shows the induction of S74 phosphorylation in WT K8 transgenic liver after OA treatment. Top panel shows K8 cross-linking (indicated by bracket) before and after OA treatment.

K8 cross-linking but robust K8 cross-linking in extracts from OA-treated cells (Fig. 3*A*). Although the HT29 extracts contain endogenous TG2 (Fig. 3*A*, bottom panel, lanes 4–6), appreciable K8 cross-linking in the cell extracts occurs only with the addition of recombinant TG2, because cellular TG2 activity is tightly regulated, and the enzyme is generally maintained in an inactive state (45–47). Our data suggest that phosphorylation at one or more Ser or Thr residues in K8 enhance its cross-linking, though phosphorylation of other proteins may also promote their cross-linking to K8.

To focus more specifically on K8 S74 phosphorylation and its potential role in K8 cross-linking, WT, S74A, and S74D K8 cDNA constructs were transiently transfected into BHK cells. *In vitro* transamidation of transfected cell extracts showed similar cross-linking for WT and S74A K8, while the phosphomimetic K8 S74D had enhanced cross-linking (Fig. 3*B*). Next, we compared the effect of the K8 S74 or Q70 mutation in transfected BHK cells on the OA-mediated enhanced transamidation that was observed in HT29 extracts. WT K8 from OA-treated cells was efficiently cross-linked after the addition of exogenous TG2 (Fig. 3*C*; compare lanes 1 and 2). In contrast, the S74A mutation greatly reduced the level of K8 cross-linking seen after OA treatment with an even higher reduction for Q70N mutation (Fig. 3*C*). Furthermore, K8 from cell extracts of isolated hepatocytes from previously described transgenic mice that express K8 S74A (30, 48) also showed a defect in TG2-mediated cross-linking *in vitro* as compared to K8 from hepatocyte extracts from transgenic mice that express WT K8 (Fig. 3*D*; compare lanes 1 and 2). In addition, hyperphosphorylation *via* exposure of the cultured primary hepatocytes to OA enhanced *in vitro* cross-linking of WT but not S74A K8. (Fig. 3*D*; lanes 1 and 3 *vs.* 2 and 4).

K8 S74A mutation inhibits keratin cross-linking and MDB formation in transgenic mice

We tested the importance of K8 S74 phosphorylation on MDB formation and keratin cross-linking *in vivo*. For this experiment, we compared susceptibility to MDB formation in mice that overexpress WT or S74A K8 along with mice that overexpress the human liver disease-predisposing mutation K8 G62C, which causes a conformational change that interferes with K8 S74 phosphorylation (30, 49). As expected, DDC feeding resulted in a robust MDB response in WT K8 mice,

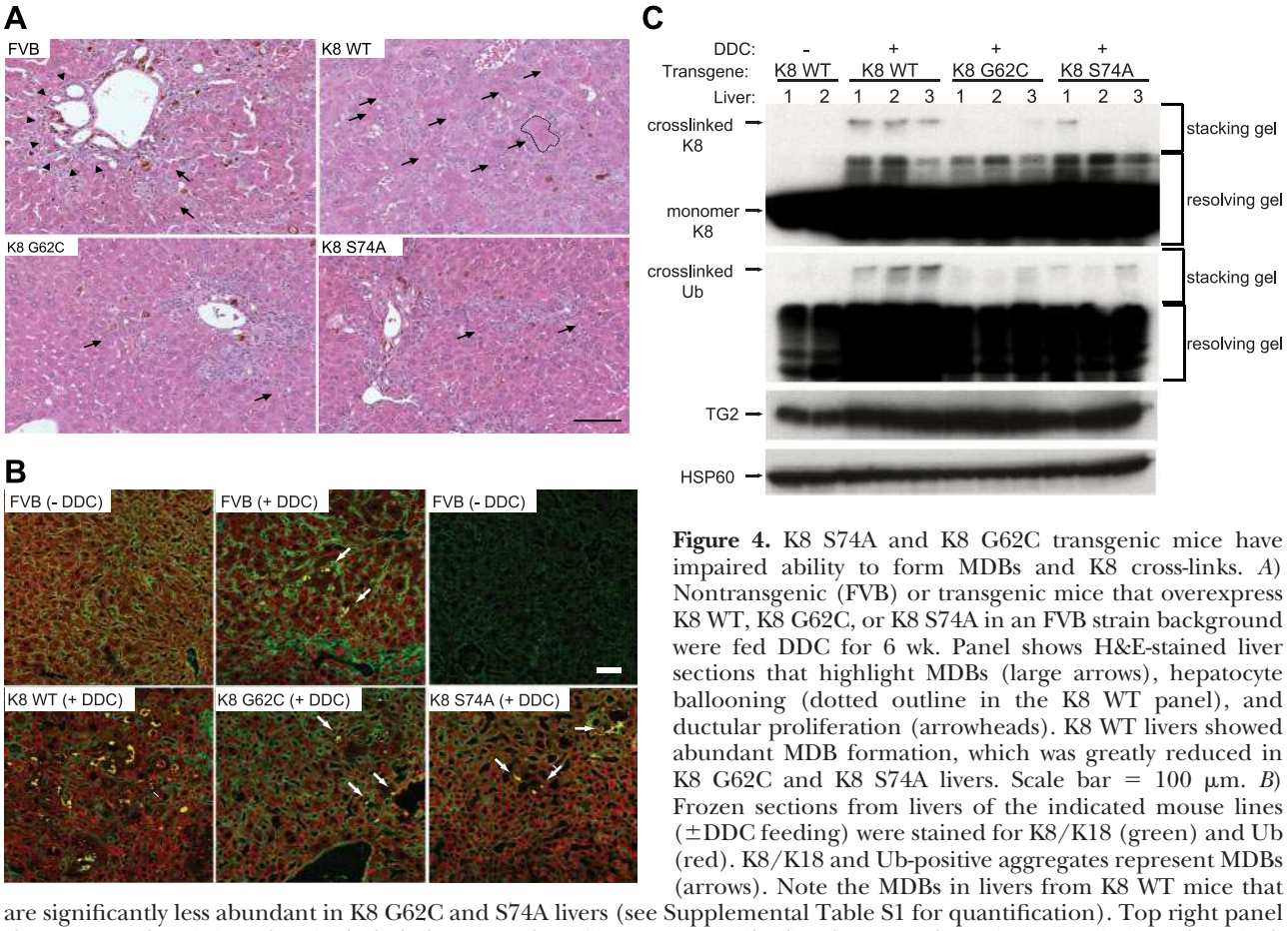

Figure 4. K8 S74A and K8 G62C transgenic mice have impaired ability to form MDBs and K8 cross-links. *A*) Nontransgenic (FVB) or transgenic mice that overexpress K8 WT, K8 G62C, or K8 S74A in an FVB strain background were fed DDC for 6 wk. Panel shows H&E-stained liver sections that highlight MDBs (large arrows), hepatocyte ballooning (dotted outline in the K8 WT panel), and ductular proliferation (arrowheads). K8 WT livers showed abundant MDB formation, which was greatly reduced in K8 G62C and K8 S74A livers. Scale bar = 100 μm. *B*) Frozen sections from livers of the indicated mouse lines (±DDC feeding) were stained for K8/K18 (green) and Ub (red). K8/K18 and Ub-positive aggregates represent MDBs (arrows). Note the MDBs in livers from K8 WT mice that are significantly less abundant in K8 G62C and S74A livers (see Supplemental Table S1 for quantification). Top right panel shows control staining that included the secondary fluorescent antibodies but not the primary anti-K8 and anti-Ub antibodies. Scale bar = 50 μm. *C*) Equal liver protein homogenates from the indicated mouse lines were blotted with antibodies to the indicated antigens. Each of the lanes represents an independent liver homogenate. Note that DDC feeding results in increased levels of TG2. The HSP60 blot serves as a loading control.

which are predisposed to MDB formation because of K8 overexpression (11, 12) as compared with nontransgenic FVB mice (**Fig. 4*A*, *B*** and Supplemental Table S1). In contrast, the MDB response (as determined by H&E and immune staining) in the K8 S74A mice was markedly inhibited while that of the K8 G62C mice was also inhibited but to a lesser extent (Fig. 4*A*, *B*; Supplemental Table S1). In addition, K8 S74A transgenic mouse liver sections contained significantly fewer ballooned hepatocytes, which are typically found in association with MDB formation (Supplemental Table S1). Other aspects of DDC-induced hepatotoxicity were assessed in the different mouse lines, including serum alanine aminotransferase, alkaline phosphatase, and total bilirubin (Supplemental Table S2), but we were not able to link any observed differences to MDB formation *per se*, given that the K8 G62C and S74A mutations play several additional roles, such as predisposition to apoptosis (30). Biochemical evidence of MDB formation, or lack thereof, was also confirmed by immunoblotting the liver homogenates with antibodies to K8 and Ub, which demonstrated the presence of K8/Ub-containing high-molecular weight complexes primarily in K8 WT livers (Fig. 4*C*).

DISCUSSION

Our findings identify Q70 as the first K8 transamidation site to be characterized, and provide evidence that mutation of K8 Q70 significantly inhibits the ability of K8 to be efficiently cross-linked by TG2 in cultured cells and *in vitro*. Notably, findings herein show that K8 Q70 is a poor TG2 substrate unless the adjacent K8 S74 becomes phosphorylated, which occurs in the context of liver injury. This scenario is consistent with the observation that K8 S74 is phosphorylated *in vivo* by the stress-activated kinases p38 (50) and JNK (51). K8 S74 phosphorylation plays several additional roles, including a phosphate sponge role that endows K8/K18 the ability to serve as stress proteins (30, 48) and a role allowing K8 and K18 filaments to reorganize in response to stress (50), which may expose several typically masked K8 rod domain lysines to sumoylation during oxidative stress and liver injury (52). Our model (**Fig. 5**) suggests that K8 S-74 phosphorylation acts as a switch that promotes TG2-mediated transamidation of K8 Q70 (and possibly other glutamines), thus initiating the process of K8 cross-linking and MDB formation. Notably, K8 Q70 is conserved in all human type II keratins and in mammalian K8 orthologs (rats, mice, pigs, and cattle), thereby supporting its potential relevance in the keratins that also have a K8 Ser74 equivalent (53). Furthermore, K8 Ser74 is conserved in several mammalian species (mice, humans, pigs, cattle, and chimpanzees), but interestingly it is replaced by Asn in rats, which can nevertheless develop MDBs in a nonalcoholic steatohepatitis model (54). In the context of rat K8, we hypothesize that other phosphorylation sites that functionally mimic mouse and human K8 S74 are likely to be involved in MDB formation in rats. Although our data suggest that Q70 might play an important role in MDB formation, they do not preclude the possibility that other K8 Gln/Lys might be important for K8 cross-linking and MDB formation. Interestingly, TG2 plays other cross-linking roles during liver injury, including the inactivation of the transcription factor Sp1 that, in turn, promotes apoptosis (55). However, it is not known whether Sp1 phosphorylation promotes cross-linking by TG2, and the potential role of phosphorylation in the regulation of TG2 cross-linking of its substrates is poorly understood. Taken

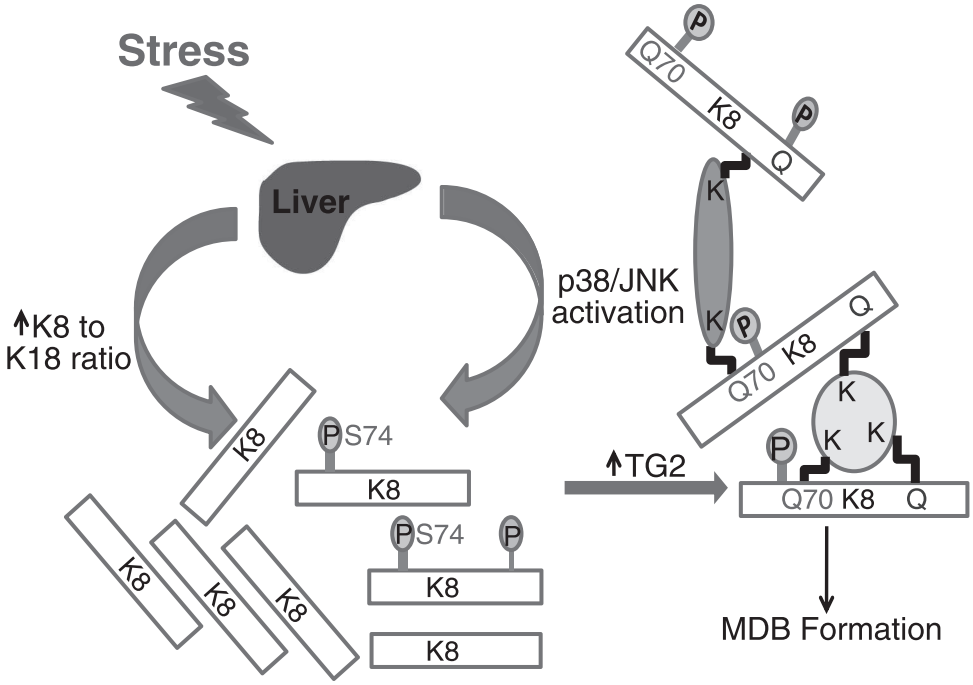

Figure 5. Model for K8 phosphorylation-modulated, TG2-mediated, K8 cross-linking, and MDB formation. Unique types of cell stress, such as DDC in mice and alcohol in humans, cause p38 and JNK kinase activation and an increase in the K8 to K18 ratio in hepatocytes. Activated p38 and JNK kinases, among others, phosphorylate K8 S74 (and S432, in addition to other potential sites represented by the label P). K8 S74 phosphorylation renders K8 Q70 (and possibly other Gln/Lys on K8 and other proteins) a good TG2 substrate, thereby leading to K8 cross-linking to other MDB constituent proteins. The increased K8 to K18 ratio and increased TG2 levels and activity in affected hepatocytes also drive the equilibrium toward K8 cross-linking and MDB formation.

together, our findings highlight a novel mechanism by which phosphorylation controls TG2-mediated transamidation and inclusion formation.

The findings herein also have potential implications for the pathogenesis of inclusions that have other IF proteins as their major constituents and whose formation is poorly understood. Examples include desmin-containing inclusions in some of the desminopathies (56), glial fibrillary acidic proteins that form inclusions termed Rosenthal fibers in Alexander disease (57), and α-internexin in neuronal intermediate filament inclusion disease (58). It remains to be determined whether phosphorylation and/or IF cross-linking *via* one or more TGs play a critical role in the formation of these inclusions. FJ

This study was supported by U.S. National Institutes of Health (NIH) grant R01 DK-52951, by the U.S. Department of Veterans Affairs (M.B.O.), and by NIH Michigan Gastrointestinal Peptide Research Center grant P30 DK34933. P.S. is supported by the Emmy Noether Program of the German Research Foundation (STR 1095/2-1). The authors are grateful to Dr. Chaitan Khosla (Stanford University, Stanford, CA, USA) for providing TG2 and thank Dr. Sujith Weerasinghe (University of Michigan) for performing mouse hepatocyte isolations.

REFERENCES

1. Zatloukal, K., French, S. W., Stumptner, C., Strnad, P., Harada, M., Toivola, D. M., Cadrin, M., and Omary, M. B. (2007) From Mallory to Mallory-Denk bodies: what, how and why? *Exp. Cell Res.* **313,** 2033–2049
2. Omary, M. B., Ku, N. O., Strnad, P., and Hanada, S. (2009) Toward unraveling the complexity of simple epithelial keratins in human disease. *J. Clin. Invest.* **119,** 1794–1805
3. Matteoni, C. A., Younossi, Z. M., Gramlich, T., Boparai, N., Liu, Y. C., and McCullough, A. J. (1999) Nonalcoholic fatty liver disease: a spectrum of clinical and pathological severity. *Gastroenterology* **116,** 1413–1419
4. Cortez-Pinto, H., Baptista, A., Camilo, M. E., and De Moura, M. C. (2003) Nonalcoholic steatohepatitis—a long-term follow-up study: comparison with alcoholic hepatitis in ambulatory and hospitalized patients. *Dig. Dis. Sci.* **48,** 1909–1913
5. Rakoski, M. O., Brown, M. B., Fontana, R. J., Bonkovsky, H. L., Brunt, E. M., Goodman, Z. D., Lok, A. S., and Omary, M. B. (2011) Mallory-Denk bodies are associated with outcomes and histological features in patients with chronic hepatitis C. *Clin. Gastroenterol. Hepatol.* **9,** 902–909
6. Strnad, P., Zatloukal, K., Stumptner, C., Kulaksiz, H., and Denk, H. (2008) Mallory-Denk-bodies: lessons from keratin-containing hepatic inclusion bodies. *Biochim Biophys Acta* **1782,** 764–774
7. Denk, H., Gschnait, F., and Wolff, K. (1975) Hepatocellar hyalin (Mallory bodies) in long-term griseofulvin-treated mice: a new experimental model for the study of hyalin formation. *Lab. Invest.* **32,** 773–776
8. Yokoo, H., Harwood, T. R., Racker, D., and Arak, S. (1982) Experimental production of Mallory bodies in mice by diet containing 3,5-diethoxycarbonyl-1,4-dihydrocollidine. *Gastroenterology* **83,** 109–113
9. Magin, T. M., Schroder, R., Leitgeb, S., Wanninger, F., Zatloukal, K., Grund, C., and Melton, D. W. (1998) Lessons from keratin 18 knockout mice: formation of novel keratin filaments, secondary loss of keratin 7 and accumulation of liver-specific keratin 8-positive aggregates. *J. Cell Biol.* **140,** 1441–1451
10. Zatloukal, K., Stumptner, C., Lehner, M., Denk, H., Baribault, H., Eshkind, L. G., and Franke, W. W. (2000) Cytokeratin 8 protects from hepatotoxicity, and its ratio to cytokeratin 18 determines the ability of hepatocytes to form Mallory bodies. *Am. J. Pathol.* **156,** 1263–1274
11. Harada, M., Strnad, P., Resurreccion, E. Z., Ku, N. O., and Omary, M. B. (2007) Keratin 18 overexpression but not phosphorylation or filament organization blocks mouse Mallory body formation. *Hepatology* **45,** 88–96
12. Nakamichi, I., Toivola, D. M., Strnad, P., Michie, S. A., Oshima, R. G., Baribault, H., and Omary, M. B. (2005) Keratin 8 overexpression promotes mouse Mallory body formation. *J. Cell Biol.* **171,** 931–937
13. Mahajan, V., Klingstedt, T., Simon, R., Nilsson, K. P., Thueringer, A., Kashofer, K., Haybaeck, J., Denk, H., Abuja, P. M., and Zatloukal, K. (2011) Cross beta-sheet conformation of keratin 8 is a specific feature of Mallory-Denk bodies compared to other hepatocyte inclusions. *Gastroenterology* **141,** 1080–1090
14. Bonar, L., Cohen, A. S., and Skinner, M. M. (1969) Characterization of the amyloid fibril as a cross-beta protein. *Proc. Soc. Exp. Biol. Med.* **131,** 1373–1375
15. Glenner, G. G., Eanes, E. D., Bladen, H. A., Linke, R. P., and Termine, J. D. (1974) Beta-pleated sheet fibrils. A comparison of native amyloid with synthetic protein fibrils. *J. Histochem. Cytochem.* **22,** 1141–1158
16. Sunde, M., and Blake, C. C. (1998) From the globular to the fibrous state: protein structure and structural conversion in amyloid formation. *Q. Rev. Biophys.* **31,** 1–39
17. Cadrin, M., Marceau, N., and French, S. W. (1992) Cytokeratin of apparent high molecular weight in livers from griseofulvin-fed mice. *J. Hepatol.* **14,** 226–231
18. Zatloukal, K., Denk, H., Lackinger, E., and Rainer, I. (1989) Hepatocellular cytokeratins as substrates of transglutaminases. *Lab. Invest.* **61,** 603–608
19. Zatloukal, K., Fesus, L., Denk, H., Tarcsa, E., Spurej, G., and Bock, G. (1992) High amount of epsilon-(gamma-glutamyl)lysine cross-links in Mallory bodies. *Lab. Invest.* **66,** 774–777
20. Denk, H., Bernklau, G., and Krepler, R. (1984) Effect of griseofulvin treatment and neoplastic transformation on transglutaminase activity in mouse liver. *Liver* **4,** 208–213
21. Riley, N. E., Li, J., Worrall, S., Rothnagel, J. A., Swagell, C., van Leeuwen, F. W., and French, S. W. (2002) The Mallory body as an aggresome: in vitro studies. *Exp. Mol. Pathol.* **72,** 17–23
22. Tazawa, J., Irie, T., and French, S. W. (1983) Mallory body formation runs parallel to gamma-glutamyl transferase induction in hepatocytes of griseofulvin-fed mice. *Hepatology* **3,** 989–1001
23. Jeitner, T. M., Bogdanov, M. B., Matson, W. R., Daikhin, Y., Yudkoff, M., Folk, J. E., Steinman, L., Browne, S. E., Beal, M. F., Blass, J. P., and Cooper, A. J. (2001) N(ε)-(γ-L-glutamyl)-L-lysine (GGEL) is increased in cerebrospinal fluid of patients with Huntington's disease. *J. Neurochem.* **79,** 1109–1112
24. Zainelli, G. M., Ross, C. A., Troncoso, J. C., and Muma, N. A. (2003) Transglutaminase cross-links in intranuclear inclusions in Huntington disease. *J. Neuropathol. Exp. Neurol.* **62,** 14–24
25. Nemes, Z., Petrovski, G., Aerts, M., Sergeant, K., Devreese, B., and Fesus, L. (2009) Transglutaminase-mediated intramolecular cross-linking of membrane-bound alpha-synuclein promotes amyloid formation in Lewy bodies. *J. Biol. Chem.* **284,** 27252–27264
26. Schmid, A. W., Chiappe, D., Pignat, V., Grimminger, V., Hang, I., Moniatte, M., and Lashuel, H. A. (2009) Dissecting the mechanisms of tissue transglutaminase-induced cross-linking of alpha-synuclein: implications for the pathogenesis of Parkinson disease. *J. Biol. Chem.* **284,** 13128–13142
27. Strnad, P., Harada, M., Siegel, M., Terkeltaub, R. A., Graham, R. M., Khosla, C., and Omary, M. B. (2007) Transglutaminase 2 regulates mallory body inclusion formation and injury-associated liver enlargement. *Gastroenterology* **132,** 1515–1526
28. Strnad, P., Siegel, M., Toivola, D. M., Choi, K., Kosek, J. C., Khosla, C., and Omary, M. B. (2006) Pharmacologic transglutaminase inhibition attenuates drug-primed liver hypertrophy but not Mallory body formation. *FEBS Lett.* **580,** 2351–2357
29. Stumptner, C., Omary, M. B., Fickert, P., Denk, H., and Zatloukal, K. (2000) Hepatocyte cytokeratins are hyperphosphorylated at multiple sites in human alcoholic hepatitis and in a mallory body mouse model. *Am. J. Pathol.* **156,** 77–90
30. Ku, N. O., and Omary, M. B. (2006) A disease- and phosphorylation-related nonmechanical function for keratin 8. *J. Cell Biol.* **174,** 115–125

31. Ku, N. O., Toivola, D. M., Zhou, Q., Tao, G. Z., Zhong, B., and Omary, M. B. (2004) Studying simple epithelial keratins in cells and tissues. *Methods Cell Biol.* **78,** 489–517
32. Scheuer, P. J. (1991) Classification of chronic viral hepatitis: a need for reassessment. *J. Hepatol.* **13,** 372–374
33. Omary, M. B., Ku, N. O., Tao, G. Z., Toivola, D. M., and Liao, J. (2006) "Heads and tails" of intermediate filament phosphorylation: multiple sites and functional insights. *Trends Biochem. Sci.* **31,** 383–394
34. Sugimura, Y., Hosono, M., Wada, F., Yoshimura, T., Maki, M., and Hitomi, K. (2006) Screening for the preferred substrate sequence of transglutaminase using a phage-displayed peptide library: identification of peptide substrates for TGASE 2 and Factor XIIIA. *J. Biol. Chem.* **281,** 17699–17706
35. Cadrin, M., French, S. W., and Wong, P. T. (1991) Alteration in molecular structure of cytoskeleton proteins in griseofulvin-treated mouse liver: a pressure tuning infrared spectroscopy study. *Exp. Mol. Pathol.* **55,** 170–179
36. Harada, M., Hanada, S., Toivola, D. M., Ghori, N., and Omary, M. B. (2008) Autophagy activation by rapamycin eliminates mouse Mallory-Denk bodies and blocks their proteasome inhibitor-mediated formation. *Hepatology* **47,** 2026–2035
37. Kachi, K., Wong, P. T., and French, S. W. (1993) Molecular structural changes in Mallory body proteins in human and mouse livers: an infrared spectroscopy study. *Exp. Mol. Pathol.* **59,** 197–210
38. Strnad, P., Tao, G. Z., So, P., Lau, K., Schilling, J., Wei, Y., Liao, J., and Omary, M. B. (2008) "Toxic memory" via chaperone modification is a potential mechanism for rapid Mallory-Denk body reinduction. *Hepatology* **48,** 931–942
39. Hanada, S., Snider, N. T., Brunt, E. M., Hollenberg, P. F., and Omary, M. B. (2010) Gender dimorphic formation of mouse Mallory-Denk bodies and the role of xenobiotic metabolism and oxidative stress. *Gastroenterology* **138,** 1607–1617
40. Shin, D. M., Jeon, J. H., Kim, C. W., Cho, S. Y., Kwon, J. C., Lee, H. J., Choi, K. H., Park, S. C., and Kim, I. G. (2004) Cell type-specific activation of intracellular transglutaminase 2 by oxidative stress or ultraviolet irradiation: implications of transglutaminase 2 in age-related cataractogenesis. *J. Biol. Chem.* **279,** 15032–15039
41. Lesort, M., Tucholski, J., Zhang, J., and Johnson, G. V. (2000) Impaired mitochondrial function results in increased tissue transglutaminase activity in situ. *J. Neurochem.* **75,** 1951–1961
42. Shin, D. M., Jeon, J. H., Kim, C. W., Cho, S. Y., Lee, H. J., Jang, G. Y., Jeong, E. M., Lee, D. S., Kang, J. H., Melino, G., Park, S. C., and Kim, I. G. (2008) TGFβ mediates activation of transglutaminase 2 in response to oxidative stress that leads to protein aggregation. *FASEB J.* **22,** 2498–2507
43. Honkanen, R. E., and Golden, T. (2002) Regulators of serine/threonine protein phosphatases at the dawn of a clinical era? *Curr. Med. Chem.* **9,** 2055–2075
44. Haystead, T. A., Sim, A. T., Carling, D., Honnor, R. C., Tsukitani, Y., Cohen, P., and Hardie, D. G. (1989) Effects of the tumour promoter okadaic acid on intracellular protein phosphorylation and metabolism. *Nature* **337,** 78–81
45. Pinkas, D. M., Strop, P., Brunger, A. T., and Khosla, C. (2007) Transglutaminase 2 undergoes a large conformational change upon activation. *PLoS Biol.* **5,** e327
46. Siegel, M., Strnad, P., Watts, R. E., Choi, K., Jabri, B., Omary, M. B., and Khosla, C. (2008) Extracellular transglutaminase 2 is catalytically inactive, but is transiently activated upon tissue injury. *PLoS One* **3,** e1861
47. Stamnaes, J., Pinkas, D. M., Fleckenstein, B., Khosla, C., and Sollid, L. M. (2010) Redox regulation of transglutaminase 2 activity. *J. Biol. Chem.* **285,** 25402–25409
48. Toivola, D. M., Strnad, P., Habtezion, A., and Omary, M. B. (2010) Intermediate filaments take the heat as stress proteins. *Trends Cell Biol.* **20,** 79–91
49. Tao, G. Z., Nakamichi, I., Ku, N. O., Wang, J., Frolkis, M., Gong, X., Zhu, W., Pytela, R., and Omary, M. B. (2006) Bispecific and human disease-related anti-keratin rabbit monoclonal antibodies. *Exp. Cell Res.* **312,** 411–422
50. Ku, N. O., Azhar, S., and Omary, M. B. (2002) Keratin 8 phosphorylation by p38 kinase regulates cellular keratin filament reorganization: modulation by a keratin 1-like disease causing mutation. *J. Biol. Chem.* **277,** 10775–10782
51. He, T., Stepulak, A., Holmstrom, T. H., Omary, M. B., and Eriksson, J. E. (2002) The intermediate filament protein keratin 8 is a novel cytoplasmic substrate for c-Jun N-terminal kinase. *J. Biol. Chem.* **277,** 10767–10774
52. Snider, N. T., Weerasinghe, S. V., Iniguez-Lluhi, J. A., Herrmann, H., and Omary, M. B. (2011) Keratin hypersumoylation alters filament dynamics and is a marker for human liver disease and keratin mutation. *J. Biol. Chem.* **286,** 2273–2284
53. Toivola, D. M., Zhou, Q., English, L. S., and Omary, M. B. (2002) Type II keratins are phosphorylated on a unique motif during stress and mitosis in tissues and cultured cells. *Mol. Biol. Cell* **13,** 1857–1870
54. de Lima, V. M., Oliveira, C. P., Alves, V. A., Chammas, M. C., Oliveira, E. P., Stefano, J. T., de Mello, E. S., Cerri, G. G., Carrilho, F. J., and Caldwell, S. H. (2008) A rodent model of NASH with cirrhosis, oval cell proliferation and hepatocellular carcinoma. *J. Hepatol.* **49,** 1055–1061
55. Tatsukawa, H., Fukaya, Y., Frampton, G., Martinez-Fuentes, A., Suzuki, K., Kuo, T. F., Nagatsuma, K., Shimokado, K., Okuno, M., Wu, J., Iismaa, S., Matsuura, T., Tsukamoto, H., Zern, M. A., Graham, R. M., and Kojima, S. (2009) Role of transglutaminase 2 in liver injury via cross-linking and silencing of transcription factor Sp1. *Gastroenterology* **136,** 1783–1795, e1710
56. Goebel, H. H. (2003) Congenital myopathies at their molecular dawning. *Muscle Nerve* **27,** 527–548
57. Liem, R. K., and Messing, A. (2009) Dysfunctions of neuronal and glial intermediate filaments in disease. *J. Clin. Invest.* **119,** 1814–1824
58. Armstrong, R. A., and Cairns, N. J. (2006) Topography of alpha-internexin-positive neuronal aggregates in 10 patients with neuronal intermediate filament inclusion disease. *Eur. J. Neurol.* **13,** 528–532

Received for publication October 19, 2011.
Accepted for publication February 7, 2012.